Copy 6
RM E53G27

NACA

RESEARCH MEMORANDUM

INVESTIGATION OF TURBINES FOR DRIVING SUPERSONIC COMPRESSORS

V - DESIGN AND PERFORMANCE OF THIRD CONFIGURATION WITH NONTWISTED ROTOR BLADES

By Warren J. Whitney, Warner L. Stewart
and Daniel E. Monroe

Lewis Flight Propulsion Laboratory
Cleveland, Ohio

NATIONAL ADVISORY COMMITTEE
FOR AERONAUTICS

WASHINGTON

September 4, 1953

NATIONAL ADVISORY COMMITTEE FOR AERONAUTICS

RESEARCH MEMORANDUM

INVESTIGATION OF TURBINES FOR DRIVING SUPERSONIC COMPRESSORS

V - DESIGN AND PERFORMANCE OF THIRD CONFIGURATION WITH NONTWISTED ROTOR BLADES

By Warren J. Whitney, Warner L. Stewart, and
Daniel E. Monroe

SUMMARY

The design and the performance are presented herein of a turbine with nontwisted rotor blades designed to drive a high-speed, high-specific-mass-flow supersonic compressor. A nontwisted-rotor velocity distribution appeared to be advantageous as compared with a free-vortex velocity distribution, because a high degree of blade-chord taper could be used without incurring three-dimensional choking inside the blade passage such as occurred for the first free-vortex turbine configuration designed for this application. The experimental results obtained on a 14-inch cold-air model of the nontwisted-rotor turbine indicated that the aerodynamic performance was satisfactory. At the design point, the turbine passed design mass flow and extracted design work at an efficiency of 0.87, which was the highest efficiency obtained. A comparison of the performance of this turbine with that of the second free-vortex turbine designed for this application indicates that both design and off-design performance of the two turbines were very nearly the same.

It was concluded from the performance results that a free-vortex velocity distribution may not always be optimum where stress as well as aerodynamics is a determining factor; and, in this particular case, diverting from a free-vortex design enabled the use of a high degree of blade taper without any apparent deterioration in over-all turbine performance. It was also concluded that a relative entrance Mach number of 0.84 at the rotor hub does not necessarily impair turbine performance if adequate passage area is provided on an over-all three-dimensional basis.

INTRODUCTION

Recent research and development of supersonic compressors have indicated the need for turbines having the characteristics of high speed and high-specific-mass flow. A turbine design for such an application is

inherently a compromise between stress and aerodynamic considerations. The investigation of turbines of this type has been the subject of an extensive program at the NACA Lewis laboratory. In reference 1 are presented the compressor characteristics and the flight conditions that were selected to define the turbine problem, together with the design and performance characteristics of the first turbine configuration designed for this application. This turbine employed a free-vortex velocity distribution and utilized a high degree of rotor-blade-chord taper to reduce the centrifugal stress. Divergence of the annulus area through the rotor, which was required because of limitations imposed by the relative rotor-entrance Mach number, was effected by means of a convex inswept rotor-blade hub. This type of contour was also used to reduce the rotor-blade centrifugal stress. The performance results obtained with this turbine showed that it failed to pass design mass flow and to extract design specific work; from the results of subsequent investigations (refs. 2 and 3), it was determined that the poor performance was due to three-dimensional flow effects that were not considered in the design procedure.

The three-dimensional analysis applied to the rotor (ref. 4) indicated that the combination of the convex hub contour and the blade-chord taper caused an effective throat to be located well within the blade passage at the hub. The effective three-dimensional throat is represented by a choking orthogonal, a curve normal to the streamlines, in a meridional plane, where choking would theoretically occur considering the three-dimensional aspects of the flow and the rotor-blade blockage effect. When the choking orthogonal occurs well inside the rotor passage, the passage operates effectively as a convergent-divergent nozzle and the design velocity diagram is not obtained. The resulting aerodynamic performance is seriously impaired, although the mass flow may or may not be appreciably reduced, depending on the passage configuration. The analysis indicated theoretically that the rotor of reference 1 would choke at less than design mass flow. From the location of the choking orthogonal, it could be expected that the tip section would reach limiting loading before the turbine limiting loading point, as discussed in reference 3. Because the analytical indications agreed well with the experimental results, it was concluded that the method of analysis, although approximate in that the assumptions of axial symmetry and inviscous isentropic flow are used, was reliable in predicting aerodynamic problems resulting from the three-dimensional character of the flow.

A second turbine was designed for this same application (ref. 5) by taking into consideration the three-dimensional flow effects. This configuration had essentially the same free-vortex velocity diagrams as did the first configuration (ref. 1) but had a concave rotor hub contour to provide more annulus area at the rotor outlet and utilized very little

blade-chord taper. The rotor-blade passage, which was designed by a two-dimensional method, was analyzed by the method of reference 4 to ascertain whether any three-dimensional aerodynamic problems would be encountered. From the results of the analysis, none were indicated. The performance results obtained with the turbine (ref. 5) indicated that aerodynamic performance was satisfactory.

In considering the aerodynamic problems encountered in the first configuration, which employed a free-vortex velocity distribution, it was determined that, aside from the convex blade hub contour, two factors contribute to the three-dimensional choking effect: (1) for a free-vortex velocity distribution, the over-all mass-flow shift is radially outward in the nozzles and radially inward in the rotor, (2) when the effect of this inward mass-flow shift combines with the effect of chordwise blade taper, the three-dimensional choking orthogonal lies inside the rotor passage near the hub. This situation was avoided to some degree in the second configuration by eliminating most of the chordwise blade taper. The average blade stress, however, for the second configuration was 80,000 as compared with 46,600 pounds per square inch for the blade of the first configuration (ref. 1). If a velocity distribution were employed in which the radial mass-flow shift is outward in the rotor, it might be possible to use a high degree of blade-chord taper without incurring serious three-dimensional choking in the passage. A velocity distribution of this type is that of a design with nontwisted rotor blades. A nontwisted rotor blade, as compared with a free-vortex blade, also appears advantageous from an induced-bending-stress consideration, since the stress induced from the overhang of the tip section is considerably reduced. A nontwisted-rotor turbine was therefore designed for this application, and its experimental performance was obtained.

The purpose of this report is to present the design and performance of the nontwisted-rotor turbine that was designed for this high-speed, high-specific-mass-flow application. The performance results are compared with those of the second free-vortex configuration of reference 5 and are used to determine whether or not the nontwisted-rotor configuration is successful in alleviating the aerodynamic problems associated with the first turbine configuration of reference 1, while still maintaining a high degree of blade-chord taper.

SYMBOLS

The following symbols are used in this report:

A_{cr}/A ratio of required critical area at Mach number of unity to required area at blade-outlet Mach number

c aerodynamic blade chord, ft

Δh specific enthalpy drop, Btu/lb

M Mach number

N rotational speed, rpm

O blade throat dimension or minimum channel width, ft

p absolute pressure, lb/sq ft

r radius, ft

s blade spacing, ft

$\Delta T'$ total temperature drop, $^{\circ}R$

U blade velocity, ft/sec

V absolute gas velocity, ft/sec

w weight-flow rate, lb/sec

α blade-outlet angle measured from tangential direction

γ ratio of specific heats

δ ratio of inlet-air total pressure to NACA standard sea-level pressure, p'/p^*

ϵ function of $\gamma, \frac{\gamma^*}{\gamma}\left[\frac{\left(\frac{\gamma+1}{2}\right)^{\frac{\gamma}{\gamma-1}}}{\left(\frac{\gamma^*+1}{2}\right)^{\frac{\gamma^*}{\gamma^*-1}}}\right]$

η adiabatic efficiency, defined as ratio of turbine work based on torque and weight-flow measurements to ideal turbine work based on inlet total temperature and inlet and outlet total pressures, both defined as consisting of static pressure plus pressure corresponding to axial component of velocity

θ_{cr} squared ratio of critical velocity at turbine inlet to critical velocity at NACA standard sea-level temperature $(V_{cr}/V^*_{cr})^2$

ρ gas density, lb/cu ft

3000

Subscripts:

cr critical

des design

r relative to rotor

t rotor tip or outer radius

u tangential component

x axial component

1 measuring station upstream of nozzles

2 measuring station at nozzle outlet, rotor inlet

3 measuring station downstream of rotor

Superscripts:

* NACA standard sea-level conditions

' total state

TURBINE DESIGN

Design Requirements

The turbine was designed to drive the same compressor as the first configuration (ref. 1). The design requirements for the cold-air turbine are the same as given in reference 1 and are included herein for convenience:

Equivalent weight flow, $\epsilon w\sqrt{\theta_{cr}}/\delta$, lb/sec	15.2
Equivalent tip speed, $U_t/\sqrt{\theta_{cr}}$, ft/sec	752
Equivalent specific enthalpy drop, $\Delta h'/\theta_{cr}$, Btu/lb	20.0

The equivalent performance requirements for the 14-inch cold-air turbine ($\gamma = 1.4$) were obtained from engine conditions ($\gamma = 1.3$) by the method of reference 6. The turbine design was based on the hot-gas conditions.

Design Procedure

Design velocity diagram. - The velocity diagrams (fig. 1(a)) were constructed by maintaining approximately the same mean-blade-span diagram as that of the first configuration (ref. 1). The nozzle-outlet velocity components at the other radii were obtained by the simplified-radial-equilibrium procedure of reference 7. The total mass flow at the nozzle outlet was obtained by integrating the point values of specific mass flow along the radius. A flow coefficient of 0.97 was assumed for the nozzle design.

At the rotor outlet, the flow was turned 5° past the axial direction at the mean blade span $(r/r_t = 0.796)$, and the axial velocity at this radial position was maintained the same as for the first configuration of reference 1. The rotor-outlet velocities at the other radii were computed by numerical integration of equation (D6) of reference 7. The simplifying assumption $U_2 = U_3$ could not be used because of the change in annular area through the rotor blade and the radial shift of mass flow. This radial streamline shift was estimated from the nozzle-outlet mass-flow distribution with the assumption of uniform mass-flow distribution $(\partial(\rho V_x)/\partial r = 0)$ at the rotor outlet. The velocities into and out of the rotor were then integrated to obtain the total work output, which was found to be 1.01 of the design work output. An over-all turbine efficiency of 0.80 was assumed in order to obtain the rotor-outlet total state. Although this efficiency might seem quite low, the design was carried out after the experimental results of the first configuration (ref. 1) were known and before the results of the second configuration (ref. 5) were known. In view of the experimental results of the first configuration, it appeared advisable to select a conservative value of efficiency and thereby provide a rotor-outlet area that is somewhat large, rather than one that is too small. The effect of assuming an efficiency value that is too low would be to cause the turbine to operate at a lower reaction than that anticipated by the design; however, the nontwisted-rotor turbine was designed to operate at a higher reaction than the second free-vortex turbine (ref. 5). A comparison of the velocity diagram (fig. 1(a)) with that of the free-vortex turbine (refs. 1 and 5) indicates that the nontwisted rotor design is not so conservative aerodynamically as the free-vortex design. The design value of the hub relative rotor-entrance Mach number for the nontwisted rotor is 0.85, which exceeds current design practice.

Nozzle-blade design. - Thirty-two blades were used in the nozzle design. The nozzle-outlet flow angle α varied from 15.8° at the tip section to 47.5° at the hub section. Because of the large change in the turning angle from hub to tip, four sectional layouts at radius ratios

of 0.67, 0.78, 0.89, and 1.00 were used in making the nozzle blade. The sections were of constant axial chord and had straight suction surfaces downstream of the nozzle throat or minimum channel width. As in reference 5, the nozzle-outlet geometry was obtained from the relation $\sin \alpha = O/s$ and was corrected for Mach numbers greater than unity by the area ratio A_{cr}/A. The nozzle-blade surfaces were laid out to obtain a passage that converged to the nozzle throat, with the suction surface faired tangent to the straight back at the throat. The curvatures of the suction and pressure surfaces were smoothed by adjusting the coordinates to obtain a continuous second derivative. The solidity c/s of the sections varied only slightly, being approximately 1.85 throughout the radial span. The nozzle blade was formed by positioning the sections so that the centers of their trailing-edge circles lay on a radial line and by fairing between the sections. The nozzle-blade coordinates are listed in table I(a).

3000

Rotor-blade design. - Twenty-nine blades were used in the rotor design. The resulting solidities were 0.9 at the tip section and 2.1 at the radius-ratio section of 0.67. Thus the solidities and the radial variation of solidity were approximately the same as for the rotor blade of the first configuration (ref. 1). Because of the taper, the blade shape varies somewhat from hub to tip. The blade was made from three sections at radius ratios of 0.67, 0.835, and 1.00; all sections had curved suction surfaces downstream of the throat, because a straight-back design would result in a very high turning rate on the suction surface of the tip section. The blade-outlet geometry was obtained from the relation $\sin \alpha = O/s$ in conjunction with a correction (ref. 8) for the curvature of the suction surface between the throat and the trailing edge. The rotor-blade surfaces were laid out to form a smoothly convergent channel, and the curvatures were smoothed in the same manner as described in the preceding section. The blade was formed by positioning the sections so as to minimize the overhang of the tip section and by fairing between the sections. The rotor-blade coordinates are given in table I(b). The inner wall through the nozzle and the rotor blading (fig. 1(b)) was faired to form a convex nozzle inner-wall contour and a concave rotor-hub contour similar to that of the second vortex turbine of reference 5.

As in reference 1, the centrifugal stress was calculated for the rotor blade by dividing the blade into strips of elemental axial width. The average blade stress was 65,000 pounds per square inch, as compared with 46,600 and 80,000 pounds per square inch for the first and second configurations, respectively.

THREE-DIMENSIONAL EFFECTS

As discussed in references 4 and 5, the effects of the three-dimensional nature of the flow should be considered in a turbine design of this type in order to obtain satisfactory performance. The radial streamline variation through the nozzle and the rotor blading was therefore estimated by using the design radial mass-flow distributions (fig. 2). From this streamline estimate, it was indicated that the rotor choking orthogonal would be located near the trailing edge of the blade in a region of the greatest annular area. Thus no three-dimensional flow problems, such as occurred for the rotor of the first configuration (ref. 1), were anticipated for this rotor design, and it was not considered necessary to analyze further the rotor passage by the method of reference 4.

From the radial streamline distribution through the nozzle blading (fig. 2), it was suspected that three-dimensional choking might occur inside the nozzle passage and reduce the mass flow from that predicted by the two-dimensional design procedure. The nozzle passage was therefore analyzed by the method of reference 4 to determine the maximum mass flow. The results of the analysis (ref. 9) indicated that the nozzles would pass a maximum mass flow of about 0.96 of design because the choking orthogonal occurred inside the passage at the inner wall (fig. 2). It was calculated that opening the nozzle blades $3\frac{1}{2}^{\circ}$ should enable the nozzles to pass design mass flow. After the nozzle blades were opened $3\frac{1}{2}^{\circ}$ and flow-tested, design mass flow was passed at the design value of nozzle total-to-static pressure ratio. The theoretical effect of the nozzle resetting on the mass average of the product U_2V_{u2} and on the rotor incidence angle was calculated, and the effect on both was found to be negligible.

APPARATUS, INSTRUMENTATION, AND METHODS

The turbine nozzle and rotor blades used in this investigation were fabricated in the same manner as described in reference 1. A photograph of the rotor assembly is shown in figure 3. The apparatus, instrumentation, and methods of calculating the performance parameters are the same as those used in reference 5. A diagrammatic sketch of the turbine rig is shown in figure 4.

The performance runs were made in the same manner as described in references 1, 2, 3, and 5, with turbine-inlet temperature and pressure maintained constant at nominal values of 135° F and 32 inches of mercury absolute, respectively. The speed was varied from 30 to 130 percent of

design speed in even increments of 10 percent. At each speed, the total-pressure ratio across the turbine was varied from approximately 2.35 to 1.35. Turbine efficiency was based on the ratio of inlet total pressure to outlet total pressure, both defined as the sum of the static pressure and the pressure corresponding to the axial component of velocity (ref. 1). Detailed radial surveys were also taken at design speed over a range of total-pressure ratios.

The accuracy of the measured and calculated parameters is estimated to be within the following limits:

Temperature, $^{\circ}F$	±0.5
Pressure, in. Hg abs	±0.05
Weight flow, percent	±1.0
Turbine speed, rpm	±20
Torque, percent design	±0.5
Efficiency, percent	±2.0

RESULTS AND DISCUSSION

The over-all turbine performance is presented in figure 5 with equivalent specific work $\Delta h'/\theta_{cr}$ shown as a function of the weight-flow - speed parameter $\epsilon w N/\delta$ for the various pressure ratios, with adiabatic efficiency η contours included. Point A on the figure represents design work and design speed; point B, the ordinate and abscissa of which were calculated from the turbine design requirements, represents design work and design weight-flow - speed parameter. Since both points A and B are actually at design speed, a comparison of the abscissas of the two points shows that the turbine did pass design weight flow. The design point A occurs in a region of highest efficiency of 0.87, which was also the highest efficiency obtained by the free-vortex turbine (ref. 5). Figure 6 presents the over-all performance of the free-vortex turbine of reference 5, which is included herein for convenience. A comparison of the two figures shows that the off-design performance of the nontwisted-rotor turbine was very nearly the same as that of the free-vortex turbine. Thus the nontwisted rotor enables the use of blade-chord taper as a stress-reduction device without any apparent sacrifice in either design or off-design performance, as compared with the performance of the free-vortex turbine.

The relative entrance Mach number at the rotor hub was calculated at design speed and design work output from the turbine-inlet total pressure, the nozzle-outlet static pressure (measured at the inner wall), and the nozzle flow angle. This angle was calculated from the circumferential average of the measured throat dimensions at the hub section

[redacted]

in conjunction with the appropriate form of the sine-law relation as given in the Design Procedure. The calculated relative entrance Mach number at the rotor hub was 0.84, as compared with the design value of 0.85. Although this Mach number would be considered too high by conventional design criteria, the experimental results indicate that turbine performance is not impaired if adequate passage area is provided.

The results of radial temperature surveys at design speed are presented in figure 7, with equivalent total-temperature-drop ratio shown as a function of rotor-outlet radius ratio. Although the curves may be somewhat in error quantitatively as a result of unsteady flow out of the rotor, their over-all trends and behavior with increasing pressure ratio are significant. Since limiting loading is a condition in which an increase in total-pressure ratio results in no further increase in work output, it is indicated on this type of plot where the temperature-drop curves at the higher pressure ratios become coincident. From these curves it can be seen that tip limiting loading does not occur up to a total-pressure ratio of 2.24. It would also appear that limiting loading might occur first at the hub section, since the temperature curves for the two highest pressure ratios appear to converge at the lowest radius ratio.

Evidence that the tip does not reach limiting loading for total-pressure ratios up to 2.3 is given by figure 8, which shows the variation of outer-shroud static pressure with axial position for various total-pressure ratios. Limiting loading would be indicated on this figure by a converging of the pressure-ratio lines at the rotor trailing edge. The fact that the static pressure at the rotor outlet continued to drop with increasing total-pressure ratio would indicate that tip limiting loading had not occurred up to a pressure ratio of 2.3. Thus, while still maintaining a high degree of blade-chord taper, the nontwisted-rotor turbine was able to operate without incurring the aerodynamic problems associated with the first free-vortex configuration.

SUMMARY OF RESULTS AND CONCLUSIONS

A nontwisted-rotor turbine with a high degree of blade-chord taper designed for high-speed, high-specific-mass-flow application has been experimentally investigated. The pertinent performance results are as follows:

1. At design speed, the turbine extracted design work at an efficiency of 0.87, which was the highest efficiency obtained.

2. At design speed and design specific-work output, the turbine passed design mass flow.

3. As indicated by the radial temperature surveys at design speed, limiting loading did not occur up to a total-pressure ratio of 2.24.

4. The turbine had very nearly the same design performance and off-design performance as the second free-vortex turbine configuration designed for this application.

5. A comparison of the performance of this turbine with that of the second free-vortex turbine would indicate that its performance was not impaired by a relative entrance Mach number of 0.84 at the rotor hub.

From the results of this investigation, it can be concluded that free-vortex velocity distribution may not always be optimum where stress as well as aerodynamics is a determining factor; and, in this particular case, diverting from a free-vortex design enabled the use of a high degree of blade taper as a stress reduction device without any apparent deterioration of turbine performance. It can also be concluded that a relative rotor-hub entrance Mach number as high as 0.84 does not necessarily impair the over-all turbine performance if adequate passage area is provided on an over-all three-dimensional basis.

Lewis Flight Propulsion Laboratory
National Advisory Committee for Aeronautics
Cleveland, Ohio, July 29, 1953

REFERENCES

1. Stewart, Warner L., Schum, Harold J., and Whitney, Warren J.: Investigation of Turbines for Driving Supersonic Compressors. I - Design and Performance of First Configuration. NACA RM E52C25, 1952.

2. Stewart, Warner L., Schum, Harold J., and Wong, Robert Y.: Investigation of Turbines for Driving Supersonic Compressors. II - Performance of First Configuration with 2.2-Percent Reduction in Nozzle Flow Area. NACA RM E52E26, 1952.

3. Stewart, Warner L., Whitney, Warren J., and Monroe, Daniel E.: Investigation of Turbines for Driving Supersonic Compressors. III - First Configuration with Four Nozzle Settings and One Nozzle Modification. NACA RM E53A20, 1953.

4. Stewart, Warner L.: Analytical Investigation of Flow Through High-Speed Mixed-Flow Turbine. NACA RM E51H06, 1951.

5. Whitney, Warren J., Stewart, Warner L., and Schum, Harold J.: Investigation of Turbines for Driving Supersonic Compressors. IV - Design and Performance of Second Configuration Including Study of Three-Dimensional Flow Effects. NACA RM E53C02, 1953.

6. Heaton, Thomas R., Slivka, William R., and Westra, Leonard F.: Cold-Air Investigation of a Turbine with Nontwisted Rotor Blades Suitable for Air Cooling. NACA RM E52A25, 1952.

7. Slivka, William R., and Silvern, David H.: Analytical Evaluation of Aerodynamic Characteristics of Turbines with Nontwisted Rotor Blades. NACA TN 2365, 1951.

8. Ainley, D. G., and Mathieson, G. C. R.: An Examination of the Flow and Pressure Losses in Blade Rows of Axial Flow Turbines. Rep. No. R. 86, British N.G.T.E., Mar. 1951.

9. Stewart, Warner L., Whitney, Warren J., and Heaton, Thomas R.: Effect of Certain Combinations of Wall Contouring and Exit Velocity Distribution on Prediction of Turbine-Nozzle Mass Flow. NACA RM E53E14, 1953.

3000

[redacted]

3000

TABLE I. - BLADE-SECTION COORDINATES FOR 14-INCH COLD-AIR TURBINE

(a) Nozzle blade.

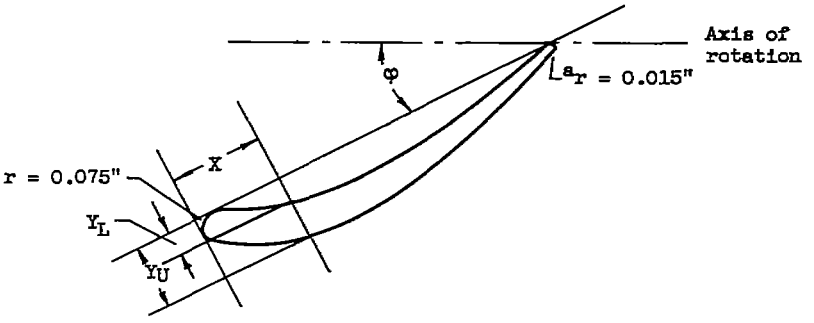

	Section radius ratio, r/r_t							
	0.67		0.78		0.89		1.00	
	φ, deg							
	23.9		36.2		45.5		52.5	
X, in.	Y_U, in.	Y_L, in.	Y_U, in.	Y_L, in.	Y_U, in.	Y_L, in.	Y_U, in.	Y_L, in.
0	0.075	0.075	0.075	0.075	0.075	0.075	0.075	0.075
.1	.185		.203		.211		.256	
.2	.235	.039	.253	.048	.280	.060	.366	.093
.3	.268	.069	.279	.083	.322	.107	.445	.172
.4	.288	.094	.291	.110	.343	.145	.502	.232
.5	.296	.114	.292	.129	.350	.173	.542	.278
.6	.296	.129	.286	.142	.348	.193	.569	.312
.7	.288	.140	.274	.149	.340	.205	.586	.337
.8	.273	.147	.258	.152	.327	.210	.592	.353
.9	.254	.149	.241	.151	.311	.210	.590	.361
1.0	.231	.146	.221	.146	.293	.205	.579	.364
1.1	.205	.138	.201	.137	.273	.195	.560	.361
1.145	.193	-----	-----	-----	-----	-----	-----	-----
1.168	(b)	-----	.187	-----	-----	-----	-----	-----
1.2		.125	(b)	.126	.252	.183	.533	.353
1.227		-----		-----	.246	-----	-----	-----
1.3		.107		.113	(b)	.169	.500	.341
1.337		-----		-----		-----	.485	-----
1.4		.085		.099		.154	(b)	.325
1.5		.059		.084		.138		.306
1.6		.032		.068		.121		.285
1.7				.050		.103		.261
1.723	.015	.015		-----		-----		-----
1.8				.031		.085		.236
1.9				.011		.066		.208
1.953			.015	.015		-----		-----
2.0						.047		.180
2.1						.027		.150
2.2						.007		.120
2.246					.015	.015		-----
2.3								.088
2.4								.056
2.5								.022
2.582							.015	.015

NACA

[a]Sections stacked over center of trailing-edge circle.
[b]Suction surface is straight from this point to point of tangency with trailing-edge radius.

[redacted]

TABLE I. - CONCLUDED. BLADE-SECTION COORDINATES FOR 14-INCH COLD-AIR TURBINE

(b) Rotor blade.

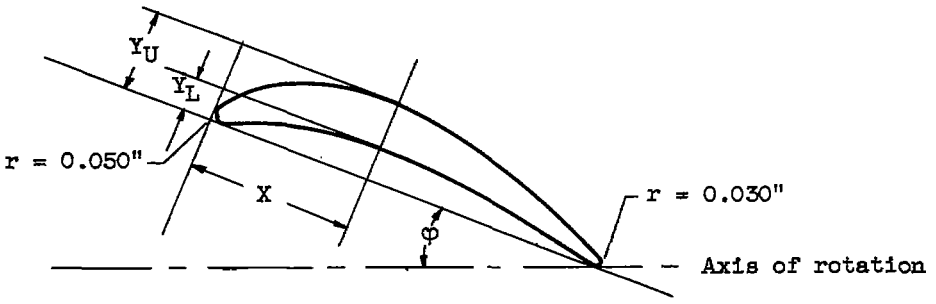

	Section radius ratio, r/r_t					
	0.67		0.835		1.00	
	Stacking-point coordinates, in.					
	X = 1.147, Y = 0.391		X = 0.942, Y = 0.318		X = 0.750, Y = 0.250	
	φ, deg					
	16.2		20.1		26.0	
X, in.	Y_U, in.	Y_L, in.	Y_U, in.	Y_L, in.	Y_U, in.	Y_L, in.
0	0.050	0.050	0.050	0.050	0.050	0.050
.1	.163	.018	.170	.021	.181	.024
.2	.236	.058	.247	.071	.255	.087
.3	.297	.097	.303	.114	.300	.134
.4	.346	.133	.344	.150	.326	.165
.5	.385	.165	.371	.179	.335	.182
.6	.414	.192	.387	.198	.331	.185
.7	.434	.214	.392	.211	.317	.176
.8	.447	.231	.388	.215	.292	.159
.9	.452	.242	.377	.212	.260	.136
1.0	.449	.247	.359	.202	.222	.110
1.1	.440	.247	.334	.185	.181	.081
1.2	.424	.240	.305	.163	.135	.049
1.3	.403	.229	.268	.136	.086	.013
1.375	-----	-----	-----	-----	.030	.030
1.4	.377	.211	.228	.107		
1.5	.347	.188	.184	.075		
1.6	.313	.162	.134	.041		
1.7	.275	.133	.079	.007		
1.755	-----	-----	.030	.030		
1.8	.232	.103				
1.9	.185	.071				
2.0	.133	.038				
2.1	.077	.004				
2.151	.030	.030				

NACA

[redacted]

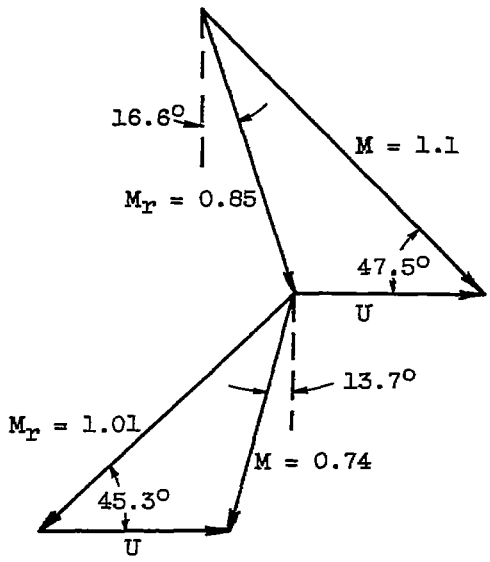

Section at r/r_t = 0.67

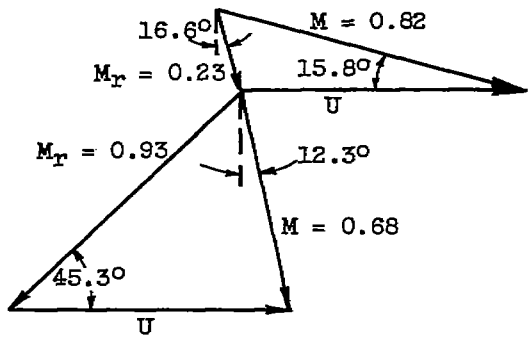

Tip section at r/r_t = 1.0

(a) Velocity diagrams.

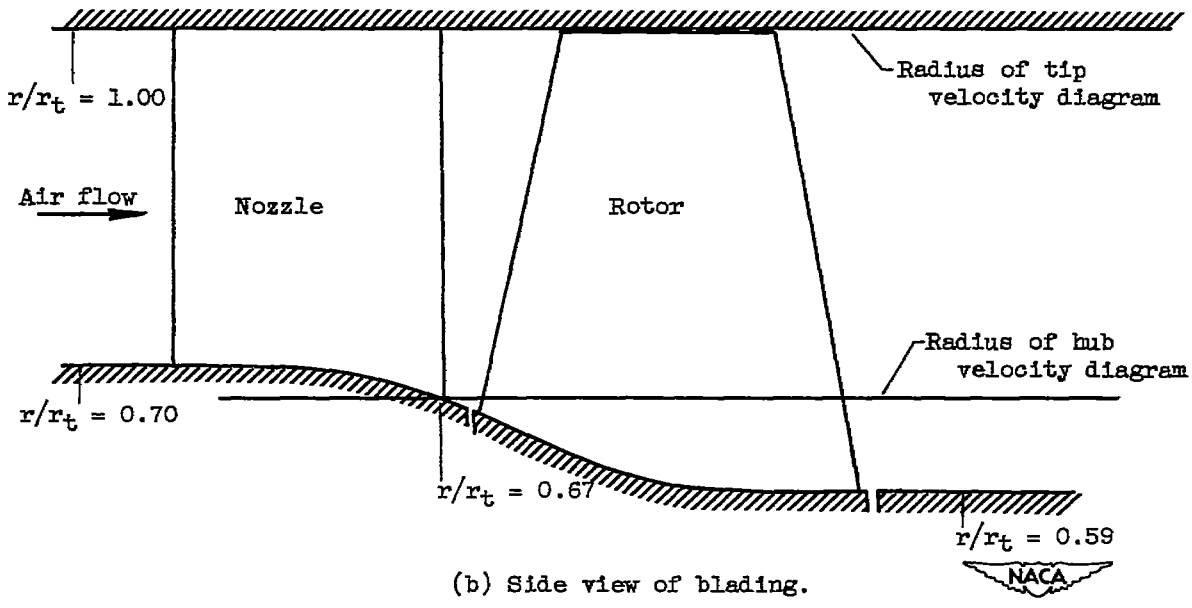

(b) Side view of blading.

Figure 1. - Design characteristics of turbine.

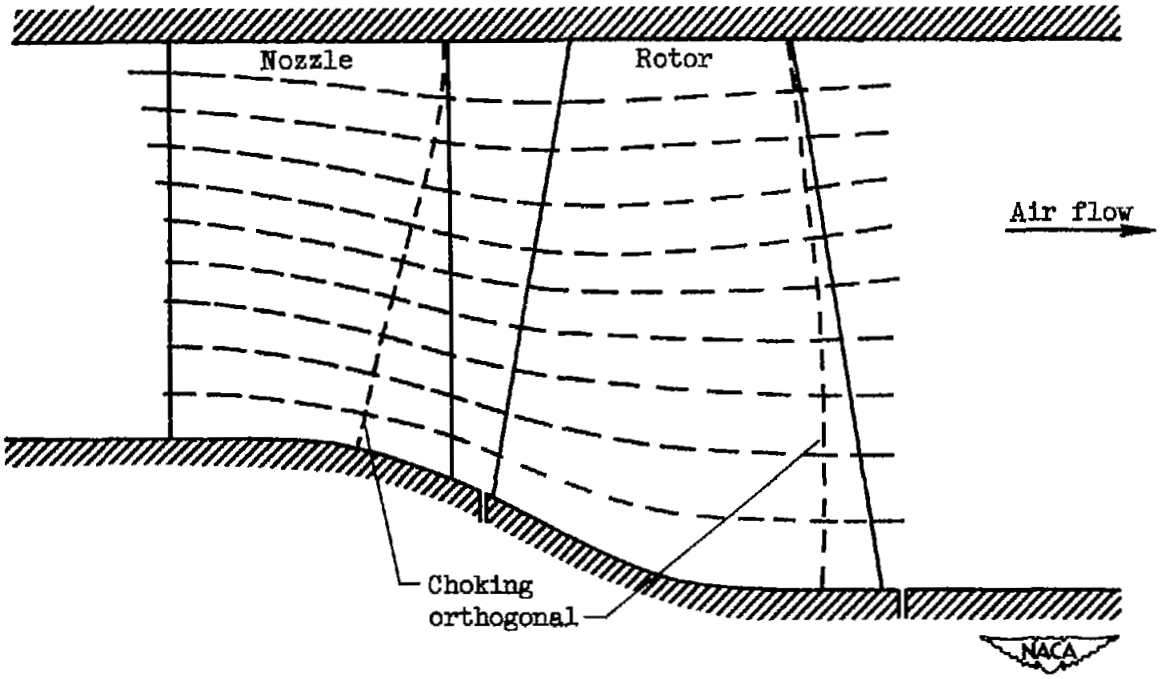

Figure 2. - Radial streamline variation through nozzle and rotor blading.

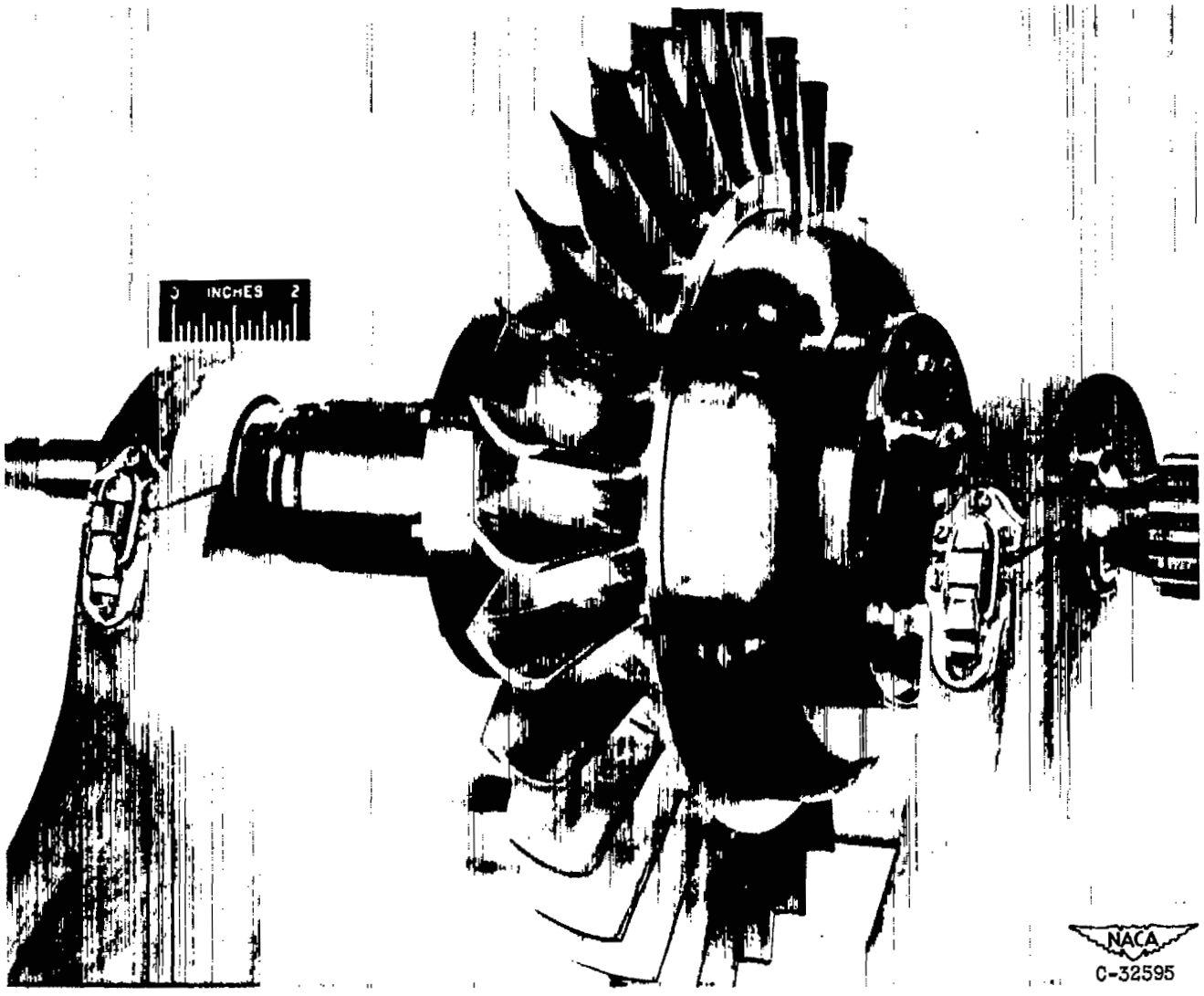

Figure 3. - Turbine rotor assembly.

3000

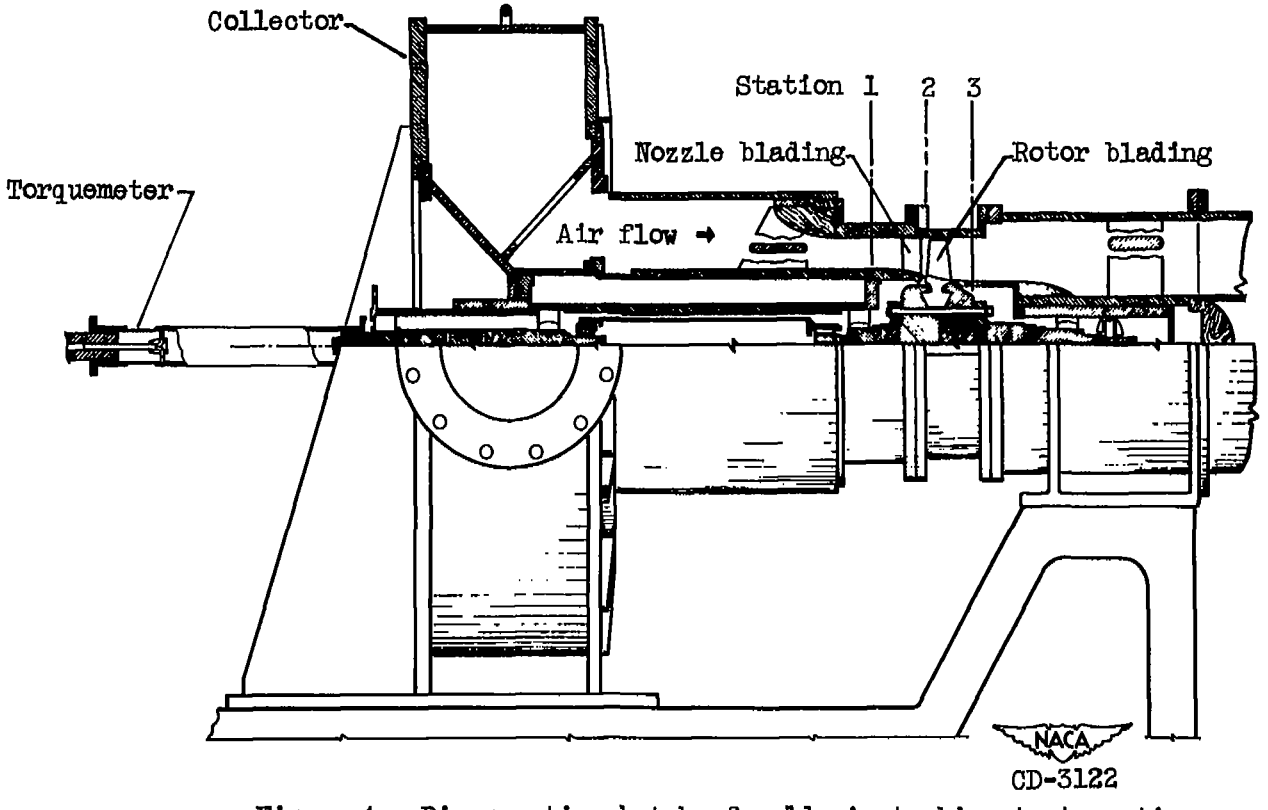

Figure 4.- Diagramatic sketch of cold-air turbine test section.

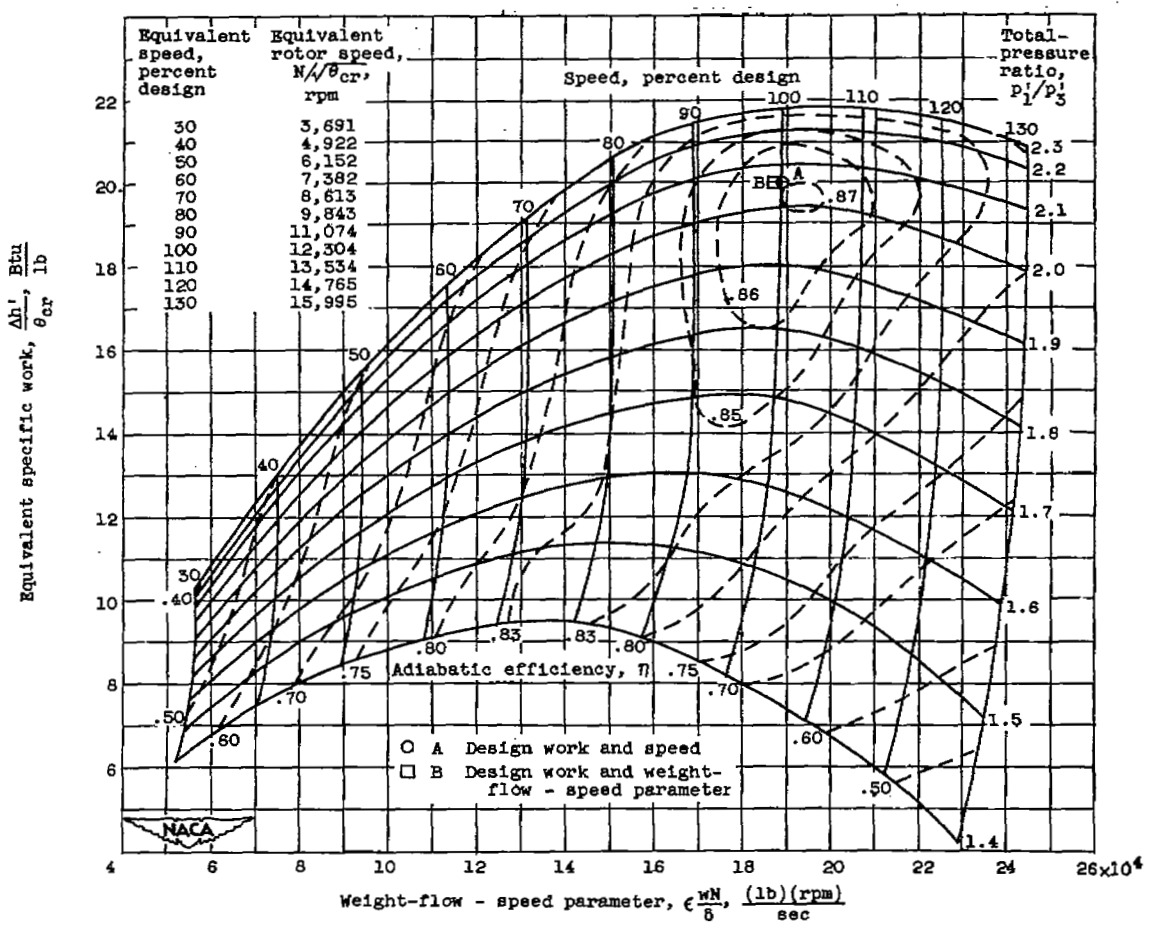

Figure 5. - Over-all performance of turbine with nontwisted rotor blades.

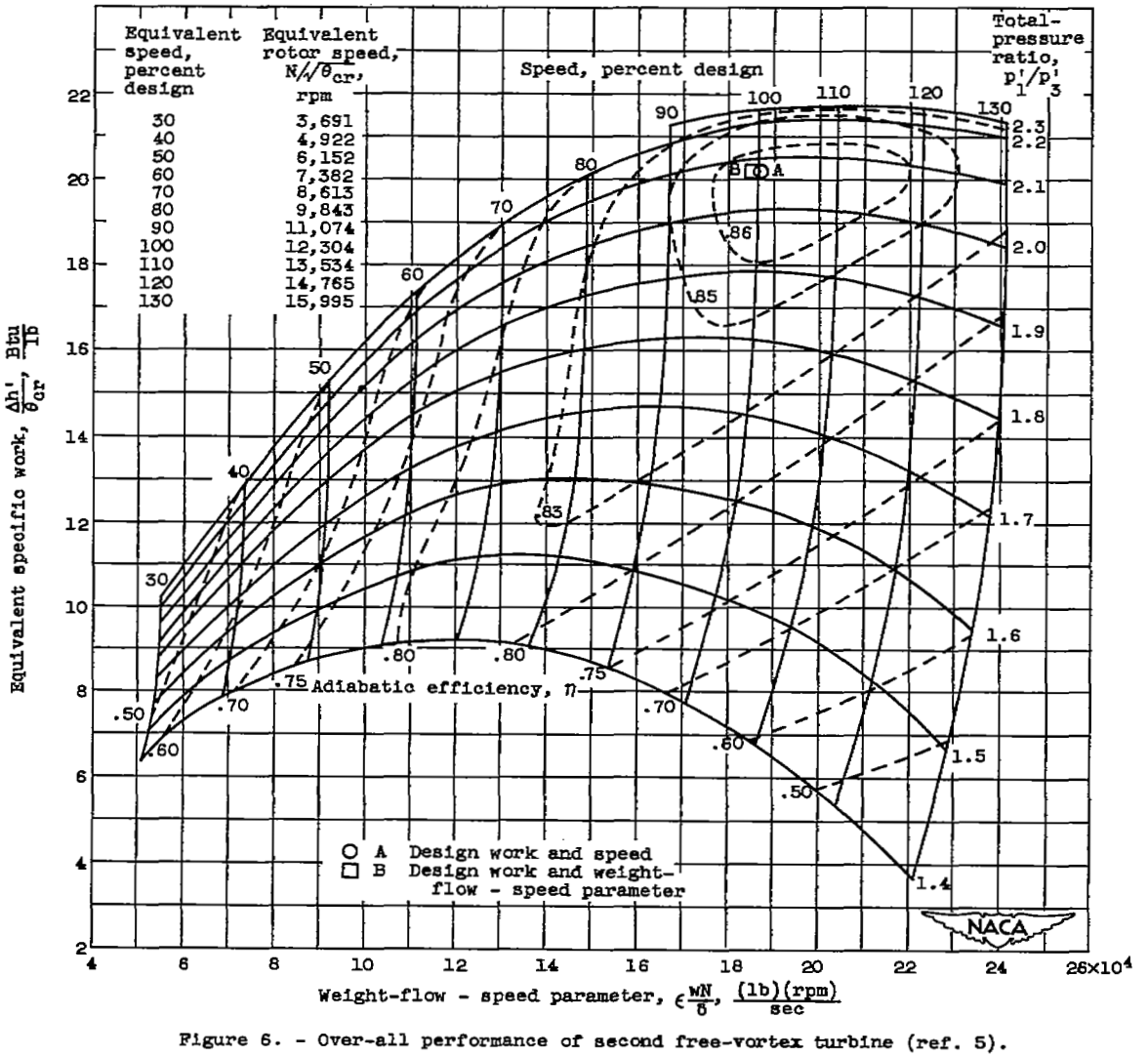

Figure 6. - Over-all performance of second free-vortex turbine (ref. 5).

[redacted]

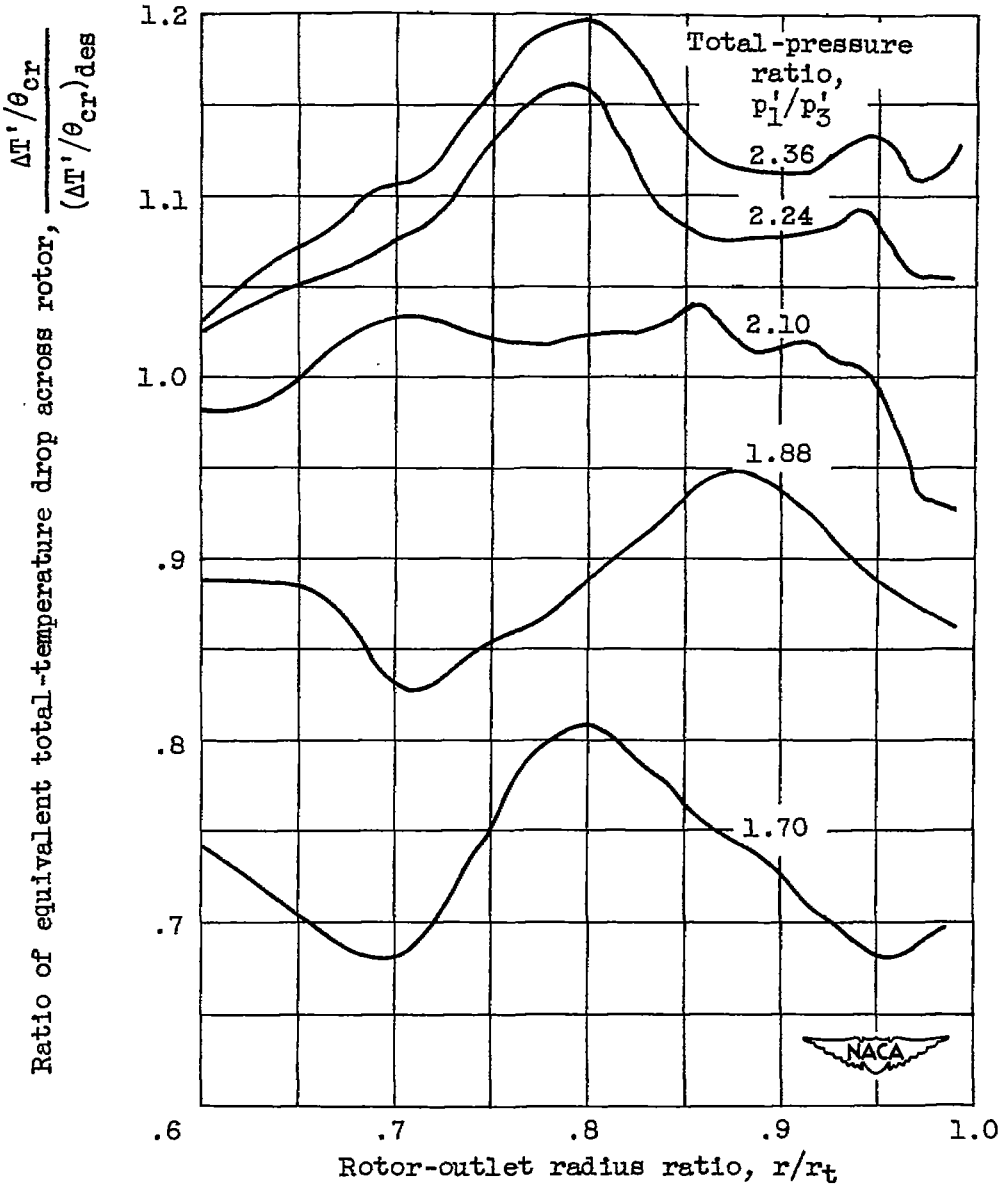

Figure 7. - Variation of equivalent total-temperature-drop ratio with rotor-outlet radius ratio at design speed for several total-pressure ratios.

3000

[redacted]

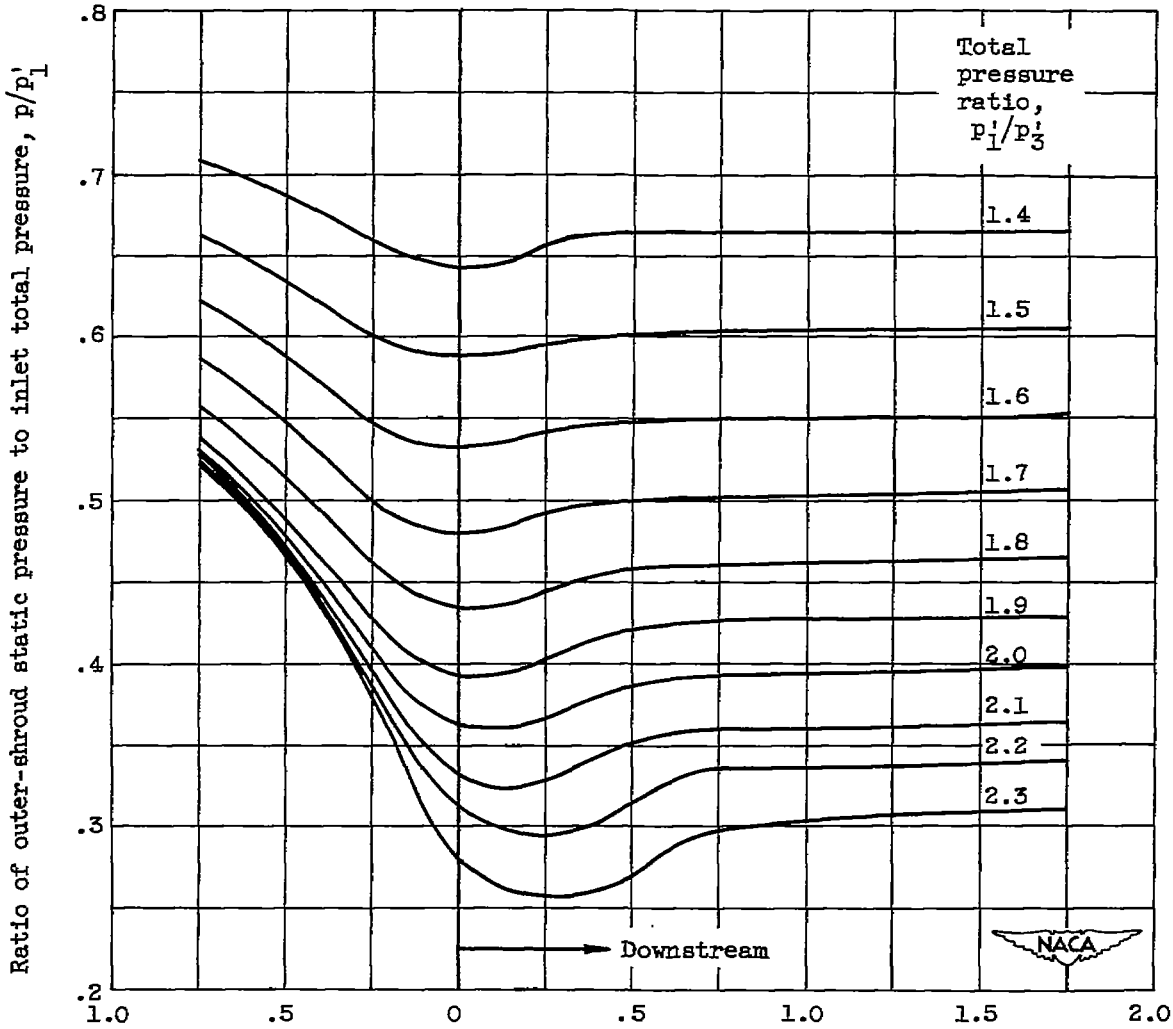

Figure 8. - Effect of turbine total-pressure ratio on outer-wall static pressure across rotor tip at design speed.